

Measurement of Upper Limits for $\Upsilon \rightarrow \gamma + \mathcal{R}$ Decays

J. L. Rosner,¹ N. E. Adam,² J. P. Alexander,² D. G. Cassel,² J. E. Duboscq,² R. Ehrlich,² L. Fields,² R. S. Galik,² L. Gibbons,² R. Gray,² S. W. Gray,² D. L. Hartill,² B. K. Heltsley,² D. Hertz,² C. D. Jones,² J. Kandaswamy,² D. L. Kreinick,² V. E. Kuznetsov,² H. Mahlke-Krüger,² P. U. E. Onyisi,² J. R. Patterson,² D. Peterson,² J. Pivarski,² D. Riley,² A. Ryd,² A. J. Sadoff,² H. Schwarthoff,² X. Shi,² S. Stroiney,² W. M. Sun,² T. Wilksen,² M. Weinberger,² S. B. Athar,³ R. Patel,³ V. Potlia,³ J. Yelton,³ P. Rubin,⁴ C. Cawfield,⁵ B. I. Eisenstein,⁵ I. Karliner,⁵ D. Kim,⁵ N. Lowrey,⁵ P. Naik,⁵ M. Selen,⁵ E. J. White,⁵ J. Wiss,⁵ R. E. Mitchell,⁶ M. R. Shepherd,⁶ D. Besson,⁷ S. Henderson,^{7,*} T. K. Pedlar,⁸ D. Cronin-Hennessy,⁹ K. Y. Gao,⁹ J. Hietala,⁹ Y. Kubota,⁹ T. Klein,⁹ B. W. Lang,⁹ R. Poling,⁹ A. W. Scott,⁹ A. Smith,⁹ P. Zweber,⁹ S. Dobbs,¹⁰ Z. Metreveli,¹⁰ K. K. Seth,¹⁰ A. Tomaradze,¹⁰ J. Ernst,¹¹ K. M. Ecklund,¹² H. Severini,¹³ W. Love,¹⁴ V. Savinov,¹⁴ O. Aquines,¹⁵ Z. Li,¹⁵ A. Lopez,¹⁵ S. Mehrabyan,¹⁵ H. Mendez,¹⁵ J. Ramirez,¹⁵ G. S. Huang,¹⁶ D. H. Miller,¹⁶ V. Pavlunin,¹⁶ B. Sanghi,¹⁶ I. P. J. Shipsey,¹⁶ B. Xin,¹⁶ G. S. Adams,¹⁷ M. Anderson,¹⁷ J. P. Cummings,¹⁷ I. Danko,¹⁷ D. Hu,¹⁷ B. Moziak,¹⁷ J. Napolitano,¹⁷ Q. He,¹⁸ J. Insler,¹⁸ H. Muramatsu,¹⁸ C. S. Park,¹⁸ E. H. Thorndike,¹⁸ F. Yang,¹⁸ T. E. Coan,¹⁹ Y. S. Gao,¹⁹ M. Artuso,²⁰ S. Blusk,²⁰ J. Butt,²⁰ J. Li,²⁰ N. Menea,²⁰ G. C. Moneti,²⁰ R. Mountain,²⁰ S. Nisar,²⁰ K. Randrianarivony,²⁰ R. Sia,²⁰ T. Skwarnicki,²⁰ S. Stone,²⁰ J. C. Wang,²⁰ K. Zhang,²⁰ G. Bonvicini,²¹ D. Cinabro,²¹ M. Dubrovin,²¹ A. Lincoln,²¹ D. M. Asner,²² K. W. Edwards,²² R. A. Briere,²³ T. Ferguson,²³ G. Tatishvili,²³ H. Vogel,²³ and M. E. Watkins²³

(CLEO Collaboration)

¹*Enrico Fermi Institute, University of Chicago, Chicago, Illinois 60637*

²*Cornell University, Ithaca, New York 14853*

³*University of Florida, Gainesville, Florida 32611*

⁴*George Mason University, Fairfax, Virginia 22030*

⁵*University of Illinois, Urbana-Champaign, Illinois 61801*

⁶*Indiana University, Bloomington, Indiana 47405*

⁷*University of Kansas, Lawrence, Kansas 66045*

⁸*Luther College, Decorah, Iowa 52101*

⁹*University of Minnesota, Minneapolis, Minnesota 55455*

¹⁰*Northwestern University, Evanston, Illinois 60208*

¹¹*State University of New York at Albany, Albany, New York 12222*

¹²*State University of New York at Buffalo, Buffalo, New York 14260*

¹³*University of Oklahoma, Norman, Oklahoma 73019*

¹⁴*University of Pittsburgh, Pittsburgh, Pennsylvania 15260*

¹⁵*University of Puerto Rico, Mayaguez, Puerto Rico 00681*

¹⁶*Purdue University, West Lafayette, Indiana 47907*

¹⁷*Rensselaer Polytechnic Institute, Troy, New York 12180*

¹⁸*University of Rochester, Rochester, New York 14627*

¹⁹*Southern Methodist University, Dallas, Texas 75275*

²⁰*Syracuse University, Syracuse, New York 13244*

²¹*Wayne State University, Detroit, Michigan 48202*

²²*Carleton University, Ottawa, Ontario, Canada K1S 5B6*

Abstract

Motivated by concerns regarding possible two-body contributions to the recently-measured inclusive $\Upsilon(nS) \rightarrow \gamma + X$ ($n=1, 2, 3$) direct photon spectra, we report on a new study of exclusive radiative decays of these narrow $\Upsilon(nS)$ resonances into two-body final states $\mathcal{R}\gamma$, with \mathcal{R} a narrow resonant hadronic state decaying into four or more charged particles. Such two-body processes are not explicitly addressed in the extant theoretical frameworks used to calculate the inclusive direct photon spectra, and must also be explicitly inserted into Monte Carlo simulations. Using data collected from the CLEO III detector at the Cornell Electron Storage Ring, we present upper limits of order 10^{-4} for such bottomonium two-body decays as a function of the recoil mass $M_{\mathcal{R}}$.

PACS numbers: 13.20.Gd,13.20.-v,13.40.Hq

*Current address: Massachusetts Institute of Technology, Cambridge, MA 02139.

Introduction

CLEO recently extracted α_s from a measurement of the direct photon spectra in $\Upsilon(1S, 2S, 3S) \rightarrow gg\gamma$ [1]. That extraction was based on a comparison of the $gg\gamma$ width to the dominant three-gluon width of the narrow bottomonium resonances. Since the direct photon is observable above background only for relatively high energies ($E_\gamma \geq E_{\text{beam}}/2$), some model dependence is inherent in the determination of the total $gg\gamma$ rate. Given a prescription relating the parton-level rate to α_s , one can then use that rate to determine α_s . To extrapolate beyond the experimentally accessible direct photon energy region, CLEO relies on theoretical parameterizations of the expected photon energy spectrum in the Υ system[2, 3] to obtain the total direct $\Upsilon \rightarrow gg\gamma$ decay width relative to the dominant $\Upsilon \rightarrow ggg$ width. The theoretical calculations are generally done at the parton level, and therefore avoid possible resonant contributions to the photon energy spectrum due to two-body decays, e.g., $\Upsilon \rightarrow gg\gamma \rightarrow \gamma\mathcal{R}$, with \mathcal{R} some resonant hadronic state. Alternatively, one would like to understand hadronization in $\Upsilon \rightarrow gg\gamma \rightarrow \gamma\mathcal{R}$, which is measured experimentally as a two-body process. For example, CLEO has recently observed signals in several low-multiplicity modes[4, 5], and has presented preliminary results consistent with the final state $\Upsilon(1S) \rightarrow \gamma + \eta'$, $\eta' \rightarrow \pi^+\pi^-\eta$, $\eta \rightarrow \pi^+\pi^-\pi^0$ [6]. We point out, however, that the product of (branching ratio) \times (efficiency) for all known exclusive modes, combined with the observed level of background, implies a signal yield below the statistical sensitivity required to be observed as a distinct signal in the inclusive spectrum.

From the experimental standpoint, the presence of possible digluon resonances opposite the photon leads to “bumps” in the otherwise smooth predicted theoretical photon spectra. The inability of the current calculations to directly address two-body effects, in part, restricts the applicability of Υ decay models to the region $z_\gamma < 0.92$, with z_γ defined as the scaled photon energy ($\equiv E_\gamma/E_{\text{beam}}$). Υ decay models are also not reliable above this point because one of the emitted gluons is of such low energy that a perturbative calculation cannot be trusted[8]. Given that primary glueball candidates are of order 1 GeV in mass, we expect the endpoint region of the photon energy spectrum ($z_\gamma > 0.92$) to be most susceptible to such contamination. Older estimates of α_s based on inclusive radiative photon production in Υ decay using the BLM[9] prescription have consistently yielded values smaller than those obtained from different techniques[7]. Recently, it has been realized that color octet contributions previously ignored in the older BLM calculation result in estimates of α_s in excellent agreement with estimates made at the Z-resonance[10]. Nevertheless, subtraction of possibly-enhanced exclusive contributions to the overall rate would, in principle, result in a lowered estimate for the ratio of rates $\Gamma(\Upsilon \rightarrow gg\gamma)/\Gamma(\Upsilon \rightarrow ggg)$ and a correspondingly larger estimate for α_s . To set the scale, given that the typical branching fraction for $\Upsilon \rightarrow gg\gamma$ is of order 10^{-2} , a total resonant enhancement at the level of 5×10^{-4} would result in a $\sim 5\%$ reduction in the estimate of α_s at the Z-pole.

By comparison, a large fraction of all $J/\psi \rightarrow gg\gamma$ decays have been identified as two-body[7]. Two-body contamination (and larger relativistic corrections) also makes the J/ψ system somewhat less reliable than the Υ in estimating α_s . This systematic consideration in the $gg\gamma$ analysis motivates our search for radiative decays of the Υ to resonances: $\Upsilon(nS) \rightarrow \gamma\mathcal{R}$ ($n=1, 2, 3$). We concern ourselves with high multiplicity (≥ 4 charged tracks) final states, as we employ the same hadronic event selection cuts in this analysis that we did in the $gg\gamma$ analysis [1]. We note that although two-body branching fractions have been observed for, e.g., $\Upsilon(1S) \rightarrow \gamma f_2(1270)$ at the level of 10^{-4} , the fraction of $f_2(1270)$ decays

into ≥ 4 charged tracks is only $\approx 3\%$ [7].

The analysis, in general terms, proceeds as follows. After selecting a high-quality sample of e^+e^- annihilations into hadrons using the hadronic event selection cuts of the previous analysis [1], we construct the inclusive isolated photon spectra in data taken at both on- Υ -resonance and off- Υ -resonance energies (the latter samples are used for systematic checks of the overall procedure). A two-body radiative decay of the Υ will produce a monochromatic photon in the lab frame; the energy of the radiated photon E_γ is related to the mass of the recoil hadron \mathcal{R} via $M_{\mathcal{R}} = 2E_{\text{beam}}\sqrt{1 - z_\gamma}$. In the case where the intrinsic width of the recoil hadron is much smaller than the experimental photon energy resolution, the measured radiative photon energy should be a Gaussian centered at the energy E_γ . For a 1 GeV (4.5 GeV) recoil photon, this implies a recoil resonance with width typically narrower than 20 MeV (260 MeV). Not knowing *a priori* the mass of the hadron \mathcal{R} , we therefore perform a set of fits of the $\Upsilon(nS)$ photon spectrum to a Gaussian signal, centered at a series of E_γ values, and with resolutions corresponding to the known CLEO III electromagnetic calorimeter resolution atop smooth polynomial backgrounds, over the range $0.2 < z_\gamma < 1.0$.¹

We construct 95% confidence level upper limits from these fits as a function of recoil mass $M_{\mathcal{R}}$, corrected for the efficiency loss due to the fiducial acceptance of the detector and the event and photon-selection cuts that define our data sample. In estimating this correction, we assume \mathcal{R} has spin=0, with a corresponding $1 + \cos^2\theta$ angular distribution for the recoil gamma; higher spins will generally give flatter angular distributions. Note that the exact form of the efficiency correction due to the event and photon selection cuts varies with the decay final states considered for \mathcal{R} . In the high-momentum region typical of the particles recoiling against the direct photon, our per-track charged particle detection efficiency is generally $\geq 90\%$ over the fiducial volume. To be conservative, we derive our z_γ -dependent efficiency correction from the decay mode yielding the worst reconstruction efficiency.

This final efficiency-corrected limit is converted into an $M_{\mathcal{R}}$ -dependent branching ratio upper limit $\mathcal{B}(\gamma\mathcal{R})$ by dividing the resulting yield by the calculated total number of resonant Υ events. For the off-resonance running, the distributions are divided by the off-resonance luminosity for the sake of comparison between continuum samples. An example of simulated signal superimposed on background is given in Figure 1 for the hypothetical process $\Upsilon(4S) \rightarrow \gamma + \mathcal{R}$, $\mathcal{R} \rightarrow \pi^+\pi^-\pi^+\pi^-$.

Event Selection

Event selection criteria in this analysis are identical to those imposed in the previous analysis [1]. The inclusive photon spectra are therefore identical to those taken from our previous analysis as well. The background shape is approximately exponential in the region

¹ It should be noted that “bumps” in the inclusive photon spectrum can be due not only to resonant two-body decays but also to continuum threshold effects such as the crossing of the $c\bar{c}$ threshold. Given our photon energy resolution, all processes of the type $e^+e^- \rightarrow D^{(*)}\bar{D}^{(*)}$ result in photons relatively close in energy and produce an apparent enhancement in the region $z_\gamma \sim 0.8$. In the previous analysis[1], we also identified an excess of photons in data as $z_\gamma \rightarrow 1$ ($\equiv E_\gamma/E_{\text{beam}}$). Further examination of these events indicated that they were dominated by continuum production: $e^+e^- \rightarrow \gamma\pi^+\pi^-\pi^+\pi^-$, although the possibility that the 4-pion state resulted from the decay of an intermediate resonance \mathcal{R} was not investigated.

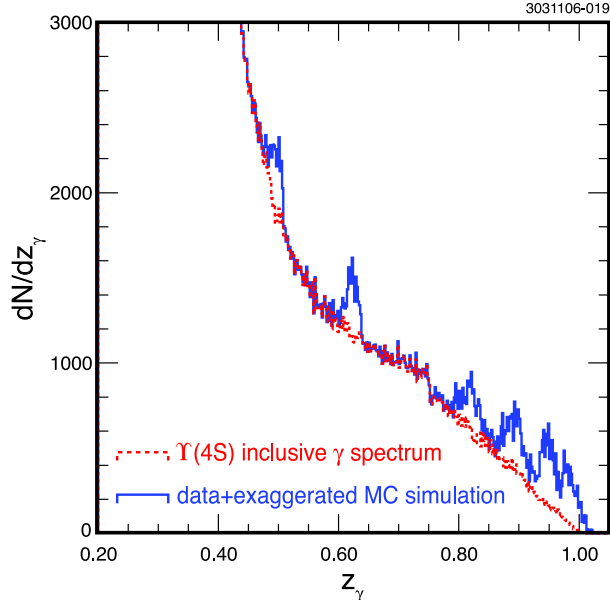


FIG. 1: Scaled photon spectrum for $\Upsilon(4S) \rightarrow \gamma\mathcal{R}$, $\mathcal{R} \rightarrow 4\pi$ simulations, for various hypothetical \mathcal{R} masses. The lower (dashed) curve is $\Upsilon(4S)$ data, while the upper (solid) curve is $\Upsilon(4S)$ data with signal Monte Carlo added on top. The magnitude of $\mathcal{B}(\Upsilon(4S) \rightarrow \gamma\mathcal{R}, \mathcal{R} \rightarrow 4\pi)$ has been grossly exaggerated for the sake of presentation ($\approx 5 \times 10^{-3}$, well above any observed radiative decay fraction into ≥ 4 charged tracks). The six elevations correspond to masses 7.5, 6.5, 4.5, 3.5, 2.5 and, for the right-most peak, the overlap of a \mathcal{R} of mass 1.5 GeV and a \mathcal{R} of mass 0.5 GeV, respectively.

$$0.2 < z_\gamma < 1.0.$$

Fitting the Inclusive Photon Spectrum

To extract the possible magnitude of a two-body radiative signal, we step along the inclusive photon spectrum over the interval $0.2 < z_\gamma < 1.0$, fitting it to a Gaussian with width equal to the detector resolution at that value of photon energy, plus a background parametrized by a smooth Chebyshev polynomial. We assume that the intrinsic width of the resonance \mathcal{R} is considerably smaller than the detector resolution. Our step size is determined by the energy resolution of the detector σ_E ; we use steps of width $\sigma_E/2$.

For photons in the central barrel ($|\cos\theta_\gamma| < 0.7$, with θ_γ the polar angle of the photon momentum vector relative to the beam axis) region of the CsI electromagnetic calorimeter, the energy resolution over the kinematic interval relevant to this analysis is of order 2%. For two-body radiative decays from the $\Upsilon(1S)$, the photon energy resolution and recoil mass resolution as a function of z_γ , are shown in Figure 2. Curves are similar for the other narrow Υ resonances.

We use a fourth-order Chebyshev polynomial to describe the background. For each fit, the Gaussian fit area $A(z_\gamma)$ and fit error $\sigma_A(z_\gamma)$ is recorded. Note that the fits are highly correlated point-to-point, and that the bin width is much finer than the detector resolution. At each step, we use a $\pm 10\sigma_E$ fitting window; the background is expected to be relatively smooth over such a limited interval.

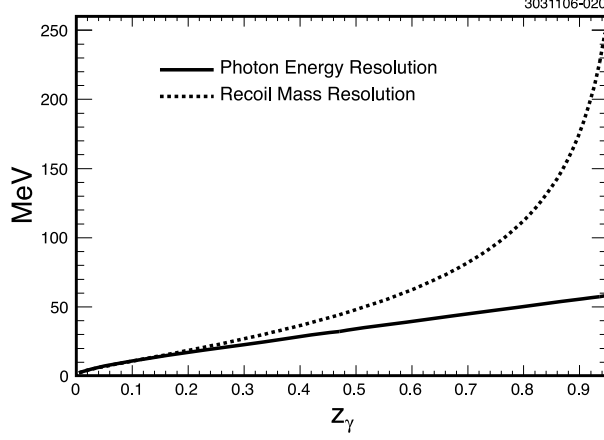


FIG. 2: Photon energy resolution (solid) and recoil mass resolution for $\Upsilon(1S) \rightarrow \gamma \mathcal{R}$ (dashed).

Extracting Upper Limits

To convert the $A(z_\gamma)$ distribution obtained from fitting the inclusive photon spectrum into a 95% confidence-interval upper limit, we add $1.645 \cdot \sigma_A(z_\gamma)$ point-wise to the $A(z_\gamma)$ distribution, as a function of photon energy. In this process, since we are interested in enhancements in the inclusive photon spectrum, all negative areas from the raw fits are set equal to zero, and the corresponding upper limit set to $1.645 \cdot \sigma_A(z_\gamma)$ at these points. The resulting contour for the $\Upsilon(1S)$ fitting is shown in Figure 3. The analogous contours for the other Υ spectra look similar.

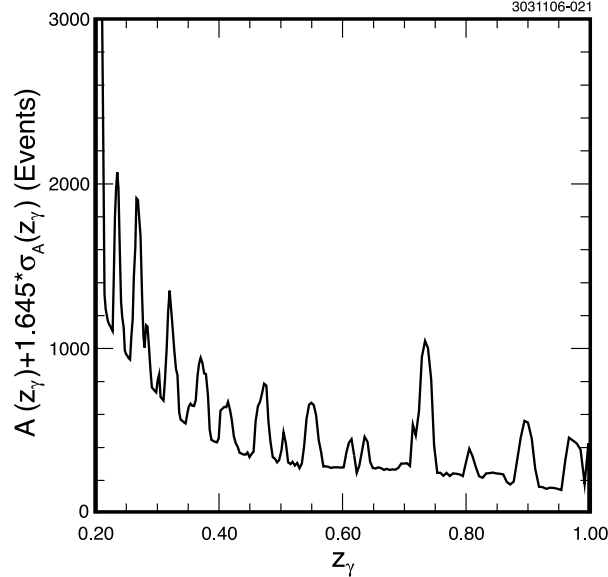


FIG. 3: $A(z_\gamma) + 1.645 \cdot \sigma_A(z_\gamma)$ versus z_γ for fits to the $\Upsilon(1S)$ inclusive photon spectrum where negative points have been mapped to $1.645 \cdot \sigma_A(z_\gamma)$. This plot is the upper limit yield, before efficiency correction, computed from statistical errors only.

We convert the limits as a function of photon energy z_γ into a function of a hypothetical resonance recoil mass $M_{\mathcal{R}}$. For the purposes of this conversion, the mean values for each

running period of E_{beam} are used for each data sample; we neglect the MeV-scale variation in beam energies for a particular run period. These values are given in Table I, along with the integrated luminosities of the resonance and below-resonance Υ data samples used in this analysis.

Event Type	E_{beam} (GeV)	\mathcal{L} (pb^{-1})
Resonance $\Upsilon(1\text{S})$	4.73	1076 ± 11
Resonance $\Upsilon(2\text{S})$	5.01	1189 ± 12
Resonance $\Upsilon(3\text{S})$	5.18	1228 ± 12
Resonance $\Upsilon(4\text{S})$	5.29	6456 ± 65
Below $\Upsilon(1\text{S})$	4.72	188 ± 2
Below $\Upsilon(2\text{S})$	5.00	396 ± 4
Below $\Upsilon(3\text{S})$	5.16	158 ± 2
Below $\Upsilon(4\text{S})$	5.27	2278 ± 23

TABLE I: The mean values of average beam energy (E_{beam}) and the integrated luminosity (\mathcal{L}) for each data sample used in this analysis.

The resulting $M_{\mathcal{R}}$ -dependent contour, for the $\Upsilon(1\text{S})$, is shown in Figure 4.

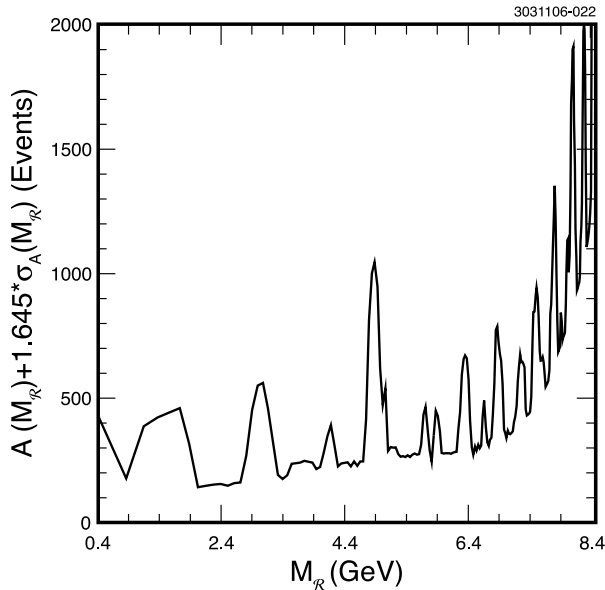


FIG. 4: $A(M_{\mathcal{R}}) + 1.645 \cdot \sigma_A(M_{\mathcal{R}})$ versus $M_{\mathcal{R}}$ for fits to the $\Upsilon(1\text{S})$ inclusive photon spectrum, where negative points have been mapped to $1.645 \cdot \sigma_A(M_{\mathcal{R}})$. Statistical errors included only.

Efficiency Correction

We consider two efficiency corrections to the upper limit contour: one due to the fiducial acceptance of the detector, and the other due to our event and shower selection cuts.

For photons in the barrel of the detector, we assume that \mathcal{R} is spin zero, which corresponds to a $1 + \cos^2 \theta$ distribution of the photons in the two-body decays we are considering; higher

spins will generally give flatter angular distributions [4]. Assuming this angular distribution amounts to an ≈ 0.6 uniform angular acceptance efficiency correction factor to our limit.

In addition to this angular acceptance correction, we assess an efficiency correction due to the CLEO III detection efficiency. Not knowing *a priori* what the decay mode of our hypothetical resonance \mathcal{R} will be, we have generated 5000-event Monte Carlo samples spanning a wide range of final state multiplicities (all with $N_{\text{charged}} \geq 4$) and masses $M_{\mathcal{R}}$. In the interests of producing a conservative upper limit, we used this study to choose the mode with the worst average efficiency. In this manner, we efficiency-correct, as a function of $M_{\mathcal{R}}$ mass, our upper limit as a function of z_{γ} (or E_{γ}) before mapping the upper limit into $M_{\mathcal{R}}$. A list of \mathcal{R} decay modes considered in this analysis and their average efficiencies (averaged over the photon energy spectrum from $1.0 \text{ GeV} \leq E_{\gamma} \leq 4.5 \text{ GeV}$) is given in Table II. We find that the worst efficiency among the decay modes considered was obtained from $\mathcal{R} \rightarrow 2(K^+K^-)\pi^0$ (Figure 5). We therefore use this efficiency function to determine our upper limit contours.

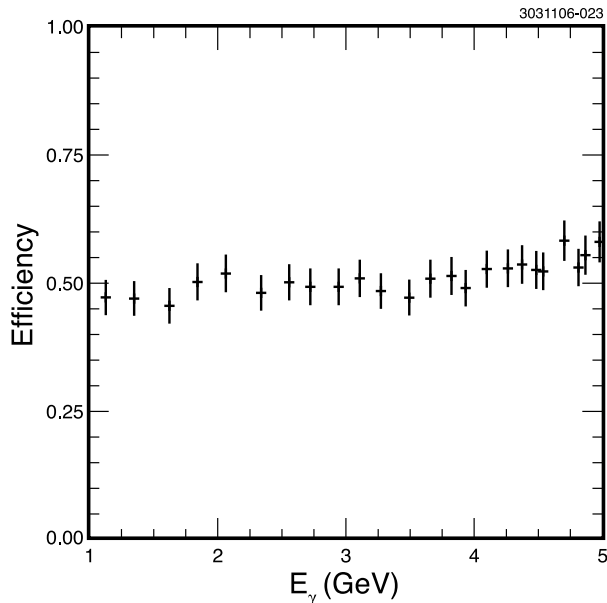


FIG. 5: The efficiency for detecting an $\Upsilon \rightarrow \gamma + \mathcal{R}$, $\mathcal{R} \rightarrow 2(K^+K^-)\pi^0$ event as a function of observed photon energy E_{γ} as determined from a 25000-event Monte Carlo sample. Each point in this efficiency is obtained from a different \mathcal{R} mass hypothesis. This photon energy-dependent efficiency correction distribution is used to point-wise correct our upper limit, where the efficiency between points in this distribution is estimated by linear interpolation.

Results

To convert the efficiency-corrected upper limit contour into an upper limit on the two-body radiative branching ratio $\mathcal{B}(\gamma\mathcal{R})$, we simply divide the efficiency-corrected upper limit contour by the total calculated number of $\Upsilon(nS)$ decays[1], as shown in Table III. For completeness, we also include the results for the $\Upsilon(4S)$, for which the decay width is expected to be nearly saturated by $\Upsilon(4S) \rightarrow B\bar{B}$ [7]. The total number of $\Upsilon(4S)$ events was obtained by multiplying the total luminosity of our on-resonance $\Upsilon(4S)$ -running by the well-known

Event Type	Average Efficiency ($\bar{\epsilon}$)
$\mathcal{R} \rightarrow K^+K^-\pi^+\pi^-$	0.53 ± 0.03
$\mathcal{R} \rightarrow K^+K^-\pi^+\pi^-\pi^0$	0.53 ± 0.02
$\mathcal{R} \rightarrow K^+K^-\pi^+\pi^-\pi^0\pi^0$	0.54 ± 0.02
$\mathcal{R} \rightarrow K^+K^-p^+p^-$	0.56 ± 0.02
$\mathcal{R} \rightarrow K^+K^-p^+p^-\pi^0$	0.50 ± 0.05
$\mathcal{R} \rightarrow K^+K^-p^+p^-\pi^0\pi^0$	0.57 ± 0.02
$\mathcal{R} \rightarrow p^+p^-\pi^+\pi^-$	0.62 ± 0.03
$\mathcal{R} \rightarrow p^+p^-\pi^+\pi^-\pi^0$	0.54 ± 0.05
$\mathcal{R} \rightarrow p^+p^-\pi^+\pi^-\pi^0\pi^0$	0.63 ± 0.02
$\mathcal{R} \rightarrow K^+K^-K^+K^-$	0.50 ± 0.02
$\mathcal{R} \rightarrow K^+K^-K^+K^-\pi^0\pi^0$	0.49 ± 0.02
$\mathcal{R} \rightarrow p^+p^-p^+p^-$	0.67 ± 0.02
$\mathcal{R} \rightarrow p^+p^-p^+p^-\pi^0$	0.65 ± 0.02
$\mathcal{R} \rightarrow p^+p^-p^+p^-\pi^0\pi^0$	0.63 ± 0.02
$\mathcal{R} \rightarrow \pi^+\pi^-\pi^+\pi^-$	0.59 ± 0.02
$\mathcal{R} \rightarrow \pi^+\pi^-\pi^+\pi^-\pi^0$	0.65 ± 0.02
$\mathcal{R} \rightarrow \pi^+\pi^-\pi^+\pi^-\pi^0\pi^0$	0.59 ± 0.01
$\mathcal{R} \rightarrow \pi^+\pi^-\pi^+\pi^-4\pi^0$	0.57 ± 0.02
$\mathcal{R} \rightarrow \pi^+\pi^-\pi^+\pi^-6\pi^0$	0.60 ± 0.02
$\mathcal{R} \rightarrow \pi^+\pi^-\pi^+\pi^-8\pi^0$	0.60 ± 0.02
$\mathcal{R} \rightarrow K^+K^-K^+K^-K^+K^-$	0.68 ± 0.04
$\mathcal{R} \rightarrow p^+p^-p^+p^-p^+p^-$	0.53 ± 0.04
$\mathcal{R} \rightarrow \pi^+\pi^-\pi^+\pi^-\pi^+\pi^-$	0.74 ± 0.03
$\mathcal{R} \rightarrow K^+K^-K^+K^-\pi^0$	0.48 ± 0.02

TABLE II: Average efficiencies for the reconstruction of various decay modes that could be detected in this analysis, obtained by fitting the photon energy-dependent reconstruction efficiencies to a straight line in the interval $1.0 \text{ GeV} < E_\gamma < 4.5 \text{ GeV}$ (statistical errors only). Quoted efficiencies correspond to 5000-event Monte Carlo samples for which photons are generated with a flat angular distribution within the barrel fiducial volume of the calorimeter, and therefore are restricted in geometry. The lowest-efficiency final state ($K^+K^-K^+K^-\pi^0$ in bold above) is used for setting upper limits.

$\Upsilon(4S)$ on-resonance cross-section (which we calculate from [11]). The resulting on-resonance upper limits $\mathcal{B}(\gamma\mathcal{R})$ are shown in Figure 6.

Given the fact that we have not performed a continuum subtraction on the on-resonance inclusive photon spectrum from Υ decays, it is interesting to compare the structure observed in Figure 6 with structure observed when we apply the fitting procedure to continuum data. Figures 7, 8, 9 and 10 show the resonances' limits of Figure 6 separately, with the corresponding continuum distributions overlaid for comparison. We observe a partial correlation between the continuum and resonance spectra, suggesting that both spectra have large contributions from initial state radiation (ISR) photons.

Applying our fitting procedure directly to the continuum we can obtain limits on the cross-section for $e^+e^- \rightarrow \gamma + \mathcal{R}$, over the barrel angular acceptance region (Figure 11).

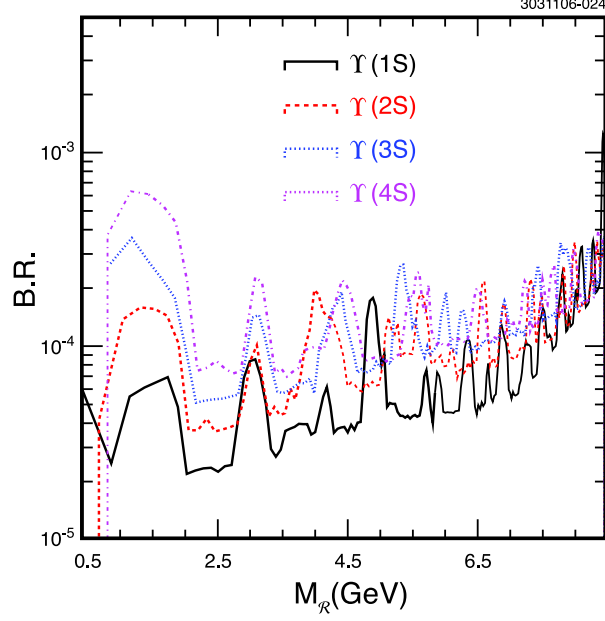


FIG. 6: The $M_{\mathcal{R}}$ -dependent $\mathcal{B}(\gamma\mathcal{R})$ upper limit contours obtained for $\Upsilon \rightarrow \gamma + \mathcal{R}$, $\mathcal{R} \rightarrow \geq 4$ charged tracks for the $\Upsilon(1S)$, $\Upsilon(2S)$, $\Upsilon(3S)$ and $\Upsilon(4S)$. Limits are obtained by dividing upper limits on yield by reconstruction efficiency and number of resonant events, and also incorporating systematic uncertainties. All limits are of order $\mathcal{B}(\gamma\mathcal{R}) \approx 10^{-4}$.

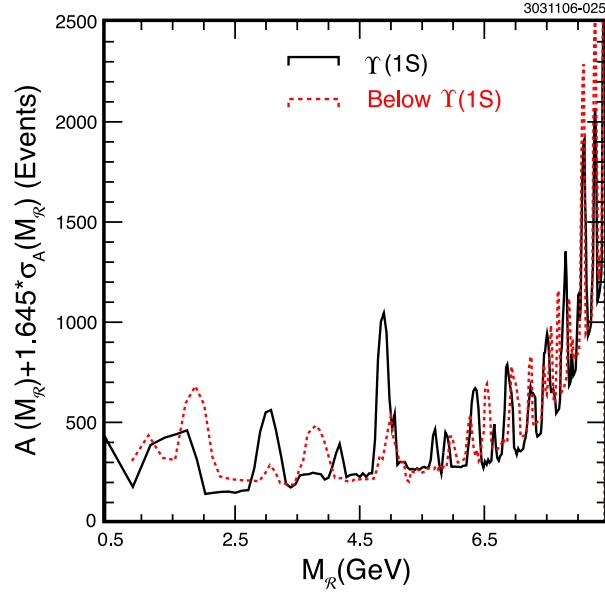


FIG. 7: Comparison of the $M_{\mathcal{R}}$ -dependent Gaussian fit area upper limit $A(M_{\mathcal{R}}) + 1.645 \cdot \sigma_A(M_{\mathcal{R}})$ for the $\Upsilon(1S)$ versus the below $\Upsilon(1S)$ continuum; we observe some correlation between the resonance and the below-resonance structure. Note that the normalization of the below-resonance upper limit curve is arbitrary and has been adjusted so as to allow an easy visual comparison.

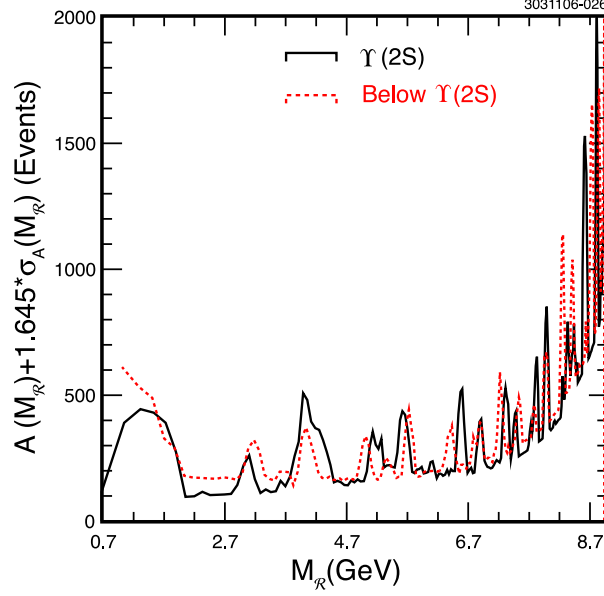


FIG. 8: Comparison of the $M_{\mathcal{R}}$ -dependent Gaussian fit area upper limit $A(M_{\mathcal{R}}) + 1.645 \cdot \sigma_A(M_{\mathcal{R}})$ for the $\Upsilon(2S)$ versus the below $\Upsilon(2S)$ continuum; scaling of the continuum as before.

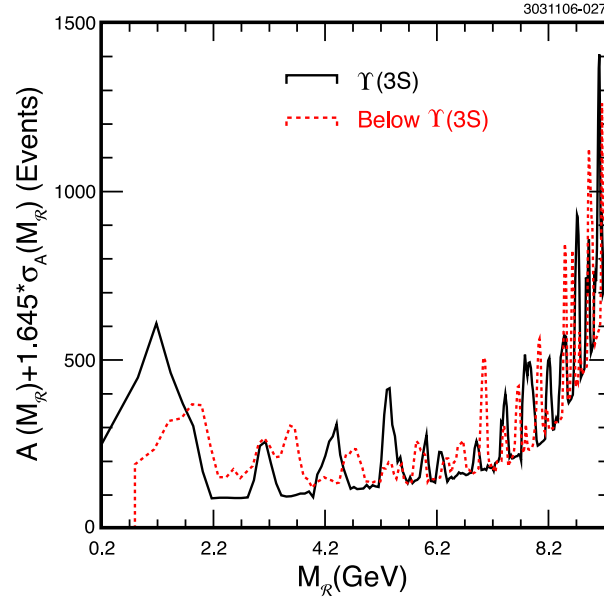


FIG. 9: Comparison of the $M_{\mathcal{R}}$ -dependent Gaussian fit area upper limit $A(M_{\mathcal{R}}) + 1.645 \cdot \sigma_A(M_{\mathcal{R}})$ for the $\Upsilon(3S)$ versus the below $\Upsilon(3S)$ continuum; scaling of the continuum as before.

It is important to note here that a) the angular distribution for continuum initial state radiation processes is considerably more forward-peaked than the $1 + \cos^2 \theta$ distribution we have assumed for the resonance; we have therefore applied a correction based on the angular distribution appropriate to ISR, and b) the quantum numbers of particles produced in association with ISR photons are different than those produced in radiative decays of quarkonium resonances. To set the scale of the continuum cross-section sensitivity, the raw ISR cross-section for $e^+e^- \rightarrow J/\psi + \gamma$ is expected to be ~ 5 pb in the 10 GeV center-of-mass

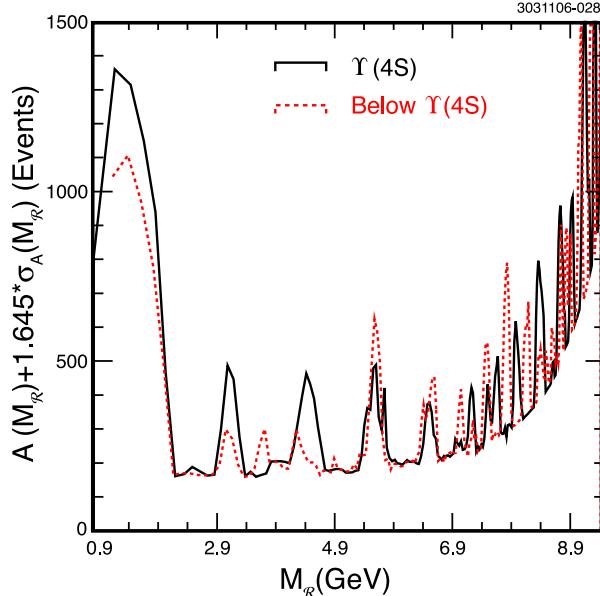


FIG. 10: Comparison of the $M_{\mathcal{R}}$ -dependent Gaussian fit area upper limit $A(M_{\mathcal{R}}) + 1.645 \cdot \sigma_A(M_{\mathcal{R}})$ for the $\Upsilon(4S)$ versus the below $\Upsilon(4S)$ continuum; scaling of the continuum as before.

Υ Resonance	$N_{\text{total}}(\Upsilon(\text{nS})) (\times 10^6)$
$\Upsilon(1S)$	20.96 ± 0.06
$\Upsilon(2S)$	8.33 ± 0.04
$\Upsilon(3S)$	5.24 ± 0.06
$\Upsilon(4S)$	6.8 ± 0.2

TABLE III: The total number of calculated $\Upsilon(1S)$, $\Upsilon(2S)$, $\Upsilon(3S)$ and $\Upsilon(4S)$ events in our data samples[1].

regime. Taking into account the efficiency of our event selection requirements and the strong forward peaking expected for ISR processes, this corresponds to an expected observed cross-section into ≥ 4 charged tracks $\sim 10^{-4}$ nb. This value is at the edge of our current statistical sensitivity.

Cross-Check

In order to check that we are able to identify a signal at a given sensitivity level, we embedded pure Monte Carlo signal into data, and performed our fitting procedure on the resulting distribution to ensure that we recover the correct signal magnitude in our branching ratio upper limit. To do this, hypothetical $\Upsilon(4S) \rightarrow \gamma + \mathcal{R}$, $\mathcal{R} \rightarrow \pi^+\pi^-\pi^+\pi^-$ events were embedded into the $\Upsilon(4S)$ inclusive photon spectrum with branching ratios of the order of 10^{-5} , 10^{-4} , 10^{-3} , and 10^{-2} under 10 different $M_{\mathcal{R}}$ hypotheses: $M_{\mathcal{R}} = 0.6$ GeV, 1.5 GeV, 2.5 GeV, 3.5 GeV, 4.5 GeV, 6.5 GeV, 7.5 GeV, 8.5 GeV, and 9.5 GeV. The resulting upper limit contours derived from applying our procedure to these spectra are show in Figure 12. We reconstruct all signals within our expected sensitivity (around 10^{-4}) that are within our

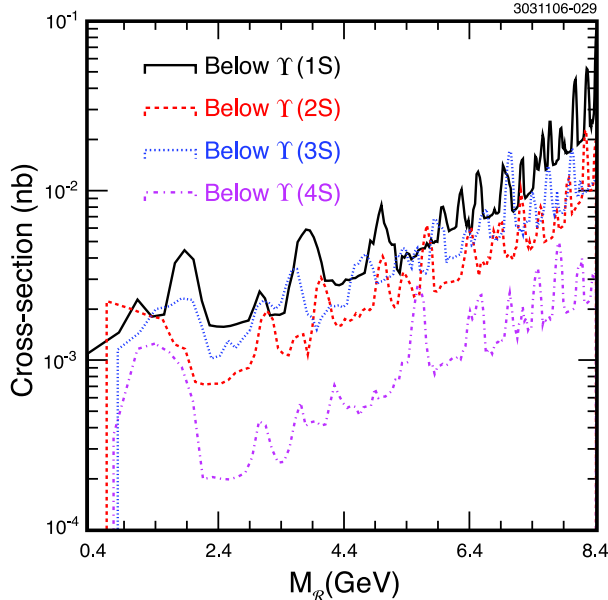


FIG. 11: $M_{\mathcal{R}}$ -dependent cross-section upper limit contours obtained for $e^+e^- \rightarrow \gamma + \mathcal{R}$, $\mathcal{R} \rightarrow \geq 4$ charged tracks for the below $\Upsilon(1S)$, $\Upsilon(2S)$, $\Upsilon(3S)$ and $\Upsilon(4S)$ continua (nb). This plot is obtained by dividing the result of our fitting procedure on the continuum by the off-resonance luminosity. The angular correction here is based on the expected distribution appropriate for continuum initial state radiation. Systematic errors have also been incorporated into these limits.

accessible recoil mass range.

Systematic errors

We identify and account for systematic errors as follows:

1. We account for possible systematics in our event and shower reconstruction efficiency by using the lowest-efficiency final state considered, and by assuming \mathcal{R} has spin=0. The angular distributions for spin=0, 1 and 2 two-body decays have been calculated, and generally yield flatter distributions for higher spins [4].
2. We have assessed fitting systematic uncertainties by varying the recoil mass bin width (from 20% to 50% of the resolution σ) and the order of the background polynomial used to parametrize the background (from second-order to fifth-order). Observing no statistically significant variation between these extremes, we have used as defaults $\sigma=5$ bins and a fourth-order background, based on the goodness of fit of the pull distributions to a unit Gaussian on the continuum.
3. For continuum measurements, we assess a uniform 1% degradation of the limit due to the luminosity uncertainty as calculated in the previous analysis [1].
4. For on-resonance measurements, we degrade the limit uniformly by the uncertainty in the calculated number of total resonant events given in Table III.

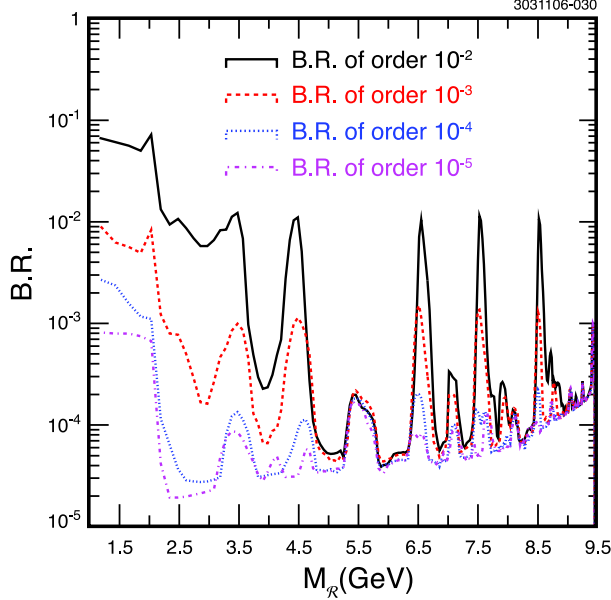


FIG. 12: Upper limit contours derived from applying our procedure to fabricated Monte Carlo signal spectra. We reconstruct all input signals withing our sensitivity ($\approx 10^{-4}$) that are within our accessible recoil mass range.

Summary

As shown in Figure 6, our sensitivity is of order 10^{-4} across the mass range corresponding to $0.2 < z_\gamma < 1.0$, well above the tabulated branching ratios for any known $\Upsilon \rightarrow \gamma + X$, $X \rightarrow h^+ h^- h^+ h^- + \text{neutrals}$ process. We measure upper limits of:

$$\begin{aligned} \mathcal{B}(\Upsilon(1S) \rightarrow \gamma + \mathcal{R}, \mathcal{R} \rightarrow \geq 4 \text{ charged tracks}) &< 1.26 \times 10^{-3}, \\ \mathcal{B}(\Upsilon(2S) \rightarrow \gamma + \mathcal{R}, \mathcal{R} \rightarrow \geq 4 \text{ charged tracks}) &< 9.16 \times 10^{-4}, \\ \mathcal{B}(\Upsilon(3S) \rightarrow \gamma + \mathcal{R}, \mathcal{R} \rightarrow \geq 4 \text{ charged tracks}) &< 9.69 \times 10^{-4} \end{aligned}$$

for all kinematically allowed masses $M_{\mathcal{R}}$, under the assumption that \mathcal{R} is a pseudoscalar. Constraining $1.5 \text{ GeV} < M_{\mathcal{R}} < 5.0 \text{ GeV}$ we set a more stringent limit of:

$$\begin{aligned} \mathcal{B}(\Upsilon(1S) \rightarrow \gamma + \mathcal{R}, \mathcal{R} \rightarrow \geq 4 \text{ charged tracks}) &< 1.78 \times 10^{-4}, \\ \mathcal{B}(\Upsilon(2S) \rightarrow \gamma + \mathcal{R}, \mathcal{R} \rightarrow \geq 4 \text{ charged tracks}) &< 1.95 \times 10^{-4}, \\ \mathcal{B}(\Upsilon(3S) \rightarrow \gamma + \mathcal{R}, \mathcal{R} \rightarrow \geq 4 \text{ charged tracks}) &< 2.20 \times 10^{-4}. \end{aligned}$$

Additionally, we report these upper limits as a function of the mass recoiling against the photon, as shown in Figure 6.

We limit the branching ratio for two-body radiative decays to narrow resonances ($< 20 \text{ MeV}$ in width) to be $\leq 10^{-4}$. We conclude that distortion of the inclusive photon spectrum in our previous extraction of α_s due to the possible contribution of such events is negligible. The possibility of resonances with widths greater than our experimental resolution has yet to be completely addressed. Further work on exclusive multiparticle final states (e.g., $\gamma 2\pi^+ 2\pi^-$, $\gamma 2K^+ 2K^-$, $\gamma K^0 K^0$ and $\gamma K^0 K^\pm \pi^\mp$) would help elucidate the nature of such radiative decays.

I. ACKNOWLEDGMENTS

We gratefully acknowledge the effort of the CESR staff in providing us with excellent luminosity and running conditions. D. Cronin-Hennessy and A. Ryd thank the A.P. Sloan Foundation. This work was supported by the National Science Foundation, the U.S. Department of Energy, and the Natural Sciences and Engineering Research Council of Canada.

- [1] D. Besson *et al.* (CLEO Collaboration), [arXiv:hep-ex/0512061], Phys. Rev. **D74**, 012003 (2006).
- [2] R.D. Field, Phys. Lett. **B133**, 248 (1983).
- [3] X. Garcia and J. Soto, [arXiv:hep-ph/0511167], Phys. Rev. Lett. **96**, 111801 (1996).
- [4] S. B. Athar *et al.* (CLEO Collaboration), [arXiv:hep-ex/0510015], Phys. Rev. **D73**, 032001 (2006).
- [5] D. Besson *et al.* (CLEO Collaboration), [arXiv:hep-ex/0512003], Phys. Rev. **D75**, 072001 (2007).
- [6] B. Athar *et al.* (CLEO Collaboration), submitted to Phys. Rev. D.
- [7] W.-M. Yao *et al.*, Journal of Physics G **33**, 1 (2006).
- [8] X. Garcia i Tormo, Ph. D. Thesis, University of Barcelona, 2007 (unpublished).
- [9] S. J. Brodsky, G. P. Lepage and P. B. Mackenzie, Phys. Rev. **D28**, 228 (1983).
- [10] N. Brambilla, X. Garcia i Tormo, J. Soto, A. Vario, [arXiv:hep-ph/0702079].
- [11] S. B. Athar *et al.* (CLEO Collaboration), [arXiv:hep-ex/0202033], Phys. Rev. **D66**, 052003 (2002).